# Design and Analysis of a Linkage-Based Wheel-Integrated Drive System

Brandon Situ[a,*], Caden Situ[b]
[a,b]Upper Canada College, M4V 1W6, Toronto, ON, Canada
[a]0009-0000-7286-4244, [b]0009-0008-0004-4886
[a]bdnsitu@gmail.com, [b]cadensitu@gmail.com

**Abstract**

Wheel-integrated drive systems incorporate the reducer, driveshaft, and constant velocity (CV) joint into the wheel, freeing space in the chassis for a battery. However, affixing the motor to the wheel increases unsprung mass. A solution is a mechanism that transmits torque via a moving parallel offset. This paper analyzes three solutions of this type (Schmidt coupling, Watt's linkage, and CV joint), each implemented in the wheel hub and driven by a motor. The angular velocity of the output shaft was determined using high-speed video at five vertical offsets of the hub center. Transmission efficiency was evaluated using stall-torque measurements at the input and output shafts, defined as the torque ratio multiplied by the gear ratio. The Schmidt coupling reduced the output velocity ripple from 71.84% to 50.12%, a 30.2% relative reduction compared to the CV joint ($p = 0.042$), while its transmission efficiency was similar to that of the CV joint ($p = 0.56$). The Watt's linkage was significantly worse than the CV joint on both measures. This suggests that a link-based mechanism can achieve fewer velocity oscillations and torque efficiency of a CV joint, thus removing the motor's mass from the unsprung wheel assembly.

**Keywords:** in-wheel drive; mechanism design; transmission efficiency; velocity ripple; wheel-integrated drive

## 1. Introduction

Wheel-integrated drive systems position the reducer, driveshaft, and constant velocity (CV) joint in the wheel. This reduces volume and cost in the chassis and allows torque and traction to be distributed to individual wheels (Deepak et al. 2023). The primary challenge to wheel-integrated drives is unsprung mass. By mounting the motor housing in the wheel hub, it is no longer suspended from the chassis, increasing the mass at each corner that the suspension must manage, with negative implications for both ride quality and grip (Mackey et al. 2017). Components mounted at the wheel are also subject to greater forces and impacts than those mounted on the chassis.

One approach to maintaining the packaging benefit while avoiding the penalty to unsprung mass is to leave the motor on the chassis and couple it to the wheel hub through some other means. This requires a coupling that transfers rotation across a parallel offset that varies as the wheel moves vertically through its suspension travel. Two such mechanisms are examined in the present study. The Schmidt coupling transfers rotation between two parallel shafts at an arbitrary offset using three discs connected through two sets of links, without requiring gears. A Watt’s linkage generates near straight-line motion using two side links and a centre link, and was modified with the addition of a gear train so that it transmits rotation as well as guiding displacement.

Both mechanisms are well established in terms of kinematics, but have not been tested in a directly comparable configuration against a CV joint as would be desirable for the application, which is the motivation for the present work. The present paper makes three contributions.

Firstly, we present a direct comparison between a Schmidt coupling, a geared Watt’s linkage, and a CV joint driven from the same wheel hub geometry and input. Secondly, transmission efficiency is determined as a function of torque ratio, de-rated by the gear ratio, which allows to abstract away from the details of the rotational speed and thus the specific motor characteristics at no load. And finally, the velocity ripple and transmission efficiency are considered jointly.

### *1.1. In-wheel drive and unsprung mass*

Deepak et al. (2023) performed a review of wheel-integrated motor drive concepts and identified unsprung mass as a key challenge, together with thermal management and sealing. These authors, as well as Mackey et al. (2017), who reach the same conclusion in an industrial context, highlight minimisation of the mass carried by the hub as the main lever for design improvement. (Xu et al. 2023) and (Zhai et al. 2022) instead address the control problem of torque distribution in four-wheel in-wheel drive rather than the mechanical design, optimising torque distribution controllers on the assumption that an in-wheel drive solution is given.
Concept vehicles have implemented multiple approaches aiming to mount the motor at a remote location. The universal wheel drive concept proposed by Hyundai Motor Group(2023) places the drive unit within the wheel while retaining a kinematic link to the chassis, without reporting efficiency or velocity ripple figures.

### *1.2. CV joint efficiency*

The CV joint is the baseline solution. Lee and Polycarpou (2010) created a phenomenological friction model of tripod CV joints based on instrumented tests at various articulation angles, oscillating speeds, lubrication conditions, and torques. They found that internal friction in a CV joint increases with articulation angle. That is, the CV joint is most efficient when aligned with the driveshaft axis and becomes progressively less efficient with suspension travel that moves it away from this alignment.

### *1.3. Parallel-offset couplings and linkage mechanisms*

Hunt (1973) analyzed the geometry of the Schmidt coupling and proved the property of constant-velocity motion analytically. Nevertheless, the authors did not evaluate the transmission efficiency or the output ripple theoretically or experimentally. Deo and Suh (2004) applied the axiomatic design methodology to a six-bar suspension linkage, also finding that the motion of the wheel is a practical design space, although it was guided rather than driven by the mechanism.

Table 1 summarises how these approaches compare with the present study.

| Study | Mechanism | Study type | Both metrics measured |
|---|---|---|---|
| Deepak et al. | In-wheel motor | Review | No |
| Mackey et al. | In-wheel motor | Experimental | No |
| Xu et al. | In-wheel motor | Simulation | No |
| Zhai et al. | In-wheel motor | Simulation | No |
| Lee and Polycarpou | CV joint | Experimental | No |
| Hunt | Schmidt coupling | Analytical | No |
| Deo and Suh | Six-bar linkage | Analytical | No |
| **This work** | **All three** | **Experimental** | **Yes** |

**Table 1.** Prior approaches compared with this work.

### *1.4. Velocity ripple*

Output smoothness is quantified as velocity ripple, the peak-to-peak variation in output angular velocity normalised by its mean over the sampling window:

$$\omega_{ripple} = (\omega_{max} - \omega_{min}) / \omega_{avg} \quad (1)$$

Normalising by the mean makes the measure independent of the absolute speed of the rig, allowing for comparison between different gear ratios.

*1.5. Torque*

Torque measurements are obtained from a force applied from a lever arm,

$$\tau = Fr = mgr \quad (2)$$

where $m$ is the mass registered at stall, $g = 9.8$ m/s$^2$, and $r$ is the lever-arm length.

*1.6. Efficiency as a speed-independent torque ratio*

Transmission efficiency is the ratio of useful output power to input power. For rotating shafts $P = \tau\omega$,

$$\eta = P_{out} / P_{in} = (\tau_{out}\omega_{out}) / (\tau_{in}\omega_{in}) \quad (3)$$

Evaluating (3) directly requires an absolute measurement of both shaft speeds under load. In a rig driven by a small DC motor this is not preferable, since the manufacturer only specifies the speed at no load, while the loaded speed has to be determined empirically. The dependence can be removed, however. For any given transmission the speed ratio is determined by its geometry, independent of the operating point. Defining the gear ratio

$$G = \omega_{in} / \omega_{out} \quad (4)$$

substitution into (3) gives

$$\eta = (1 / G) \cdot (\tau_{out} / \tau_{in}) \quad (5)$$

Equation (5) only requires two torque measurements and the ratio of the mechanism. The absolute shaft rotational speed cancels. Thus, the result does not depend on the accuracy of the motor's unloaded speed rating. The Schmidt coupling and the CV joint both transmit motion with a ratio of 1:1 so $G = 1$ and efficiency only depends on the ratio of the torques. The geared Watt's linkage incorporates an 8:1 gear train, giving $G = 8.000$. (5) was determined using the measurements at stall. Since the output power is zero at stall, (3) cannot be used to find the efficiency at stall, so instead the torque ratio is used as a substitute for the ratio of the output power to the input power. This is justified by the fact that for these two types of mechanism, the losses are predominantly Coulomb friction in the link pivots and gear flanks, for which the dependence on velocity is weak (unlike viscous and inertial losses), and therefore, to a first approximation, may be considered to be independent of velocity. Thus, the values in Table 4 are a comparison of the friction in different mechanisms under similar loading conditions, rather than a direct comparison of their running efficiencies.

## 2. Materials and Methods

*2.1. Experimental setup*

The aim of the experiment is to determine the effect of the mechanism on the performance of the wheel-hub drive, measured by the output velocity ripple and transmission efficiency. Experiments were conducted with the same hub geometry, input motor, and mounting conditions. Three types of wheel hub mechanisms were developed in computer-aided design and 3D printed: a CV joint, a geared Watt’s linkage, and a Schmidt coupling. The last two mechanisms are depicted in Figure 1. The same hubs, the same output shaft diameter, and the same printed stands were used for mounting, so the only difference between the objects under study was the mechanism.

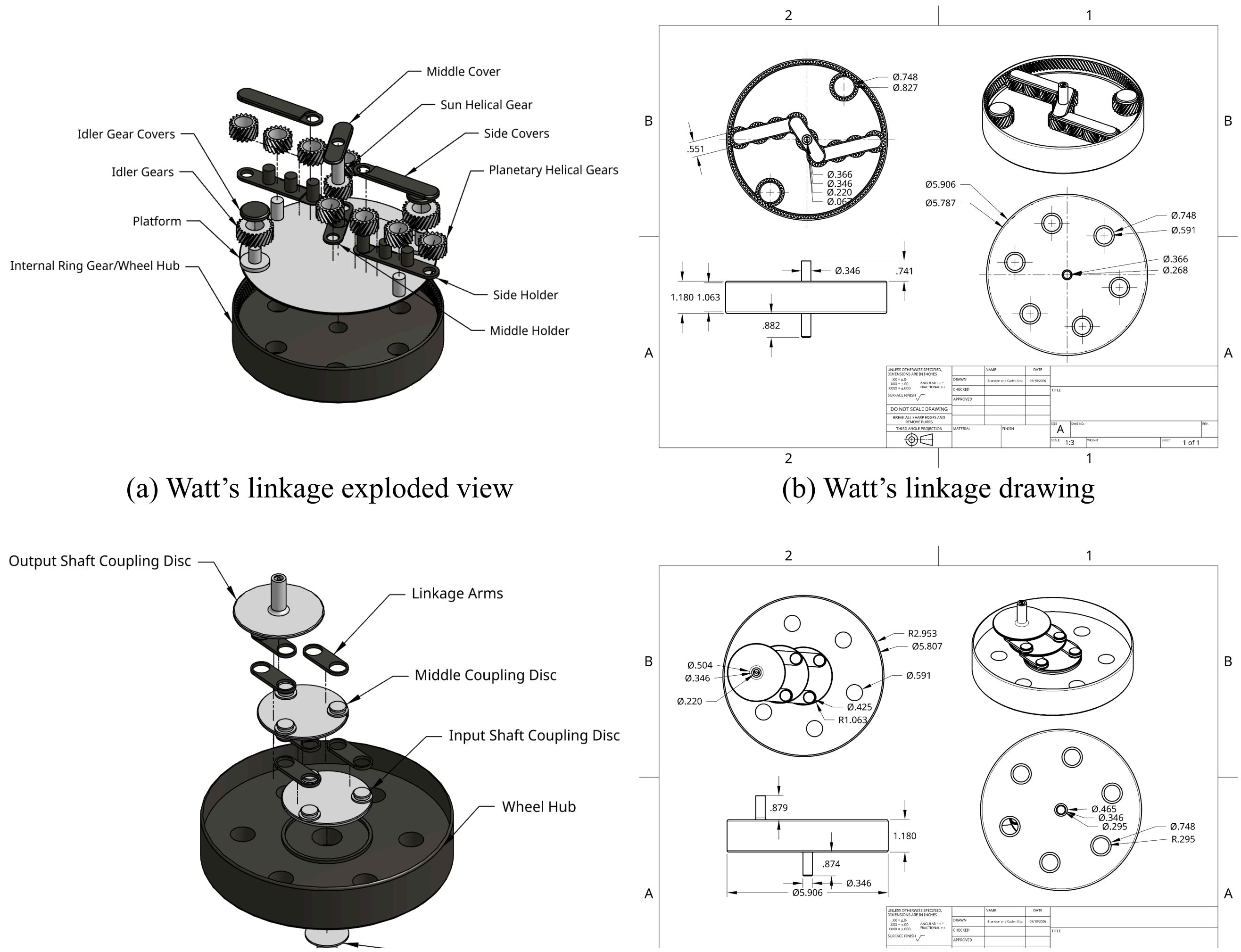


(a) Watt’s linkage exploded view

(b) Watt’s linkage drawing

**Figure 1.** 3D models and drawings of Watt’s linkage and Schmidt coupling wheel hubs.

All three were controlled by a DC gearbox motor (1:90 metal gears, 110 RPM nominal) with a TB6612FNG and an Arduino Uno. Positions were captured at 240 frames per second and digitized in the open-source program Tracker (Figure 2). Torque was measured by using a printed torque arm, a measuring scale, string, and mass. All mechanisms were tested at 5 hub vertical offsets: −3.0, −1.5, 0.0, +1.5, and +3.0 cm.

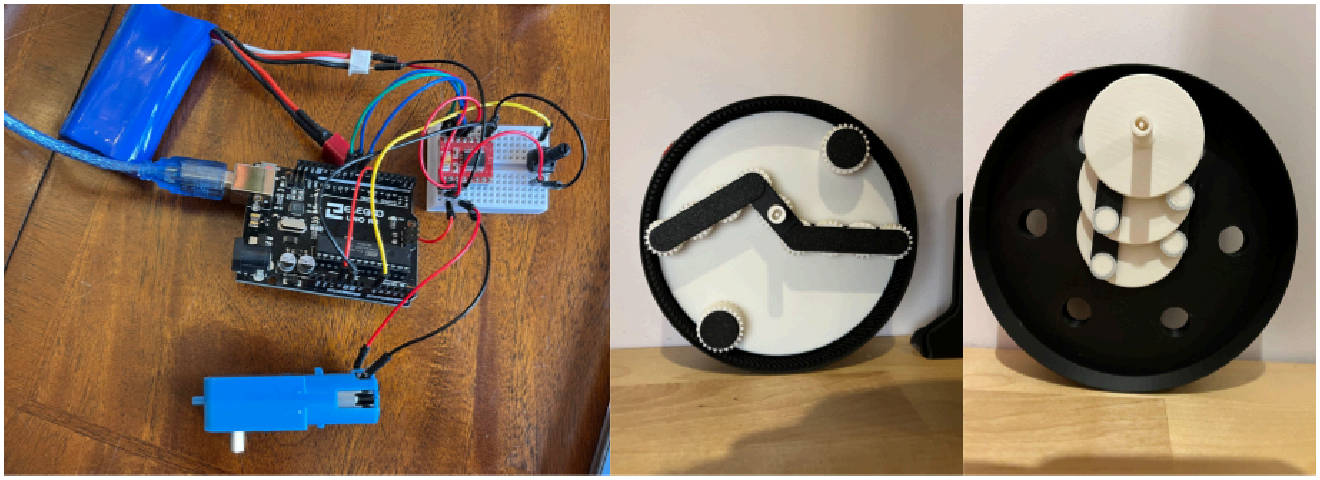

(a) Wiring setup | (b) Watt's linkage in-wheel hub motor | (c) Schmidt coupling in-wheel hub motor.

**Figure 2.** The experimental apparatus.

*2.2. Velocity ripple procedure*

A colored indicator was attached to the wheel's side. The motor was mounted to the input with the camera's field of view perpendicular to the drive shaft. The motor was accelerated to the maximum speed and allowed to run for 3 s before the wheel hub was recorded for 10 s at 240 frames/s. The video was digitized by Tracker software, frame by frame, to determine the angular position of the indicator as a function of time. The angular velocity was calculated from the difference between consecutive positions.

*2.3. Velocity validation*

Because the angular velocity is computed based on another measurement, having taken the differences, the resulting series had to be cleaned from outliers. When calculating frame-to-frame differences for a manually tracked point, it is possible to obtain extreme values for the indicator because of incorrectly indicated positions (clicking on the wrong point or clicking outside of the tracked object). For that reason, all values below zero and higher than Q3 + 1.5 IQR were removed, and the series was limited to one revolution to avoid the effects of partial periods.

The resulting mean rotational speeds were 46.1 RPM for the CV joint, 41.8 RPM for the Schmidt coupling, and 29.1 RPM for the Watt's linkage. In all cases, the value was lower than the ones predicted by the motor's 110 RPM no-load performance and the respective kinematic ratios. There are two reasons for the discrepancy. First, in all cases, the 110 RPM is the no-load speed, and the torque caused the reduction in speed, which was specific to each mechanism, without the torque being measured. Second, for the Watt's linkage, the measured speed used the mark on the hub body, not the rotating part. The angular velocity of the hub is not a fixed ratio to the angular velocity of the driven output member because of the non-linearity during the motion cycle. Therefore, the entry for the Watt's linkage in the Table 3 actually represents the speed of the hub body, not the rotating output member. It should be noted as the upper bound output ripple.

For the Schmidt coupling and the CV joint the tracked marker rotates with the output member; hence, the choice of radial position has no influence on either reported quantity. Velocity ripple is defined in Eq. (1) as the peak-to-peak variation of angular velocity about the mean, divided by that same mean value. Since both terms are scaled by an identical factor when the motion of the marker is accelerated or decelerated relative to the output shaft, this factor cancels out. Similarly, transmission efficiency is calculated from two torque measurements and the kinematic ratio (Eq. (5)) and does not depend on speed at all. Hence, the absolute velocities of the markers cited in Table 3 specify the operating point of each test, but have no direct influence on the results presented.

### *2.4. Transmission efficiency procedure*

Input torque was determined by fixing the motor level at the surface of the measuring scale, mounting the assembly on the stands, and attaching the printed torque arm to the motor shaft. Motor speed was increased using the potentiometer until the motor stalled, and the maximum mass registered on the scale was recorded. The input lever arm was $r_{in}$ = 0.05 m.

The output torque was determined by fixing the motor at the input gear, mounting the assembly on the stands, tying a string to the output wheel hub, and hanging the masses from the free end of the string. The motor was turned to the maximum and masses were added until the hub was able to lift. By hanging them, the maximum mass that could be raised was established. The output lever was $r_{out}$ = 0.075 m. For each of the five hub offsets, this procedure was repeated, as well as for each mechanism, and their efficiencies were calculated using (5).

### *2.5. Qualitative observations*

Visible vibration of the hub and associated noise were observed in all three assemblies. The noise is attributable to friction between printed gear and link surfaces despite the light lubrication that was applied. Noticeable play was observed in the gear train of the Watt's linkage, consistent with printed-part tolerance. A slight oscillation of the motor itself was also observed, meaning that the motor contributed to the ripple seen at the output. This is addressed in Section 4.6 and Section 6.4.

### *2.6. Sources of uncertainty*

The Tracker position marker resolves to ±0.1 cm, the scale to ±0.1 g, and lever arms were measured to ±0.5 mm. Propagating these through (2) and (5) in quadrature, the lever-arm term dominates the mass term by roughly twenty to one, and the combined instrument contribution to efficiency is approximately ±0.5 percentage points. Moreover, run-to-run variability creates uncertainty, arising from friction in bearings and gears, gear backlash and binding, and drift in motor speed under load. This cannot be reduced by finer instruments and is not captured by resolution figures. It was estimated as the standard error of the mean across the five hub offsets. For efficiency this is ±0.9, ±0.4, and ±1.3 percentage points for the CV joint, Watt's linkage, and Schmidt coupling respectively; for velocity ripple it is ±6.6, ±9.1, and ±6.1 percentage points. Table 2 lists the contributing factors.

| **Source** | **Type** | **Magnitude** | **Affects** |
|---|---|---|---|
| Position marker | Resolution | ±0.1 cm | Ripple |
| Mass scale | Resolution | ±0.1 g | Efficiency |
| Lever-arm length | Resolution | ±0.5 mm | Efficiency |

| Source | Type | Magnitude | Affects |
|---|---|---|---|
| Bearing, plastic, and gear friction | Variability | ±0.4–1.3 pp | Efficiency |
| Gear backlash and binding | Variability | ±0.4–1.3 pp | Efficiency |
| Motor speed | Variability | ±0.4–1.3 pp | Efficiency |

**Table 2.** Uncertainty contributions.

## 3. Results

### *3.1. Velocity ripple*

Table 3 gives the mean, maximum, and minimum output angular velocity and the resulting ripple from (1) for all three mechanisms at all five hub offsets.

| Mechanism | Offset (cm) | ωavg (°/s) | ωmax (°/s) | ωmin (°/s) | Ripple (%) |
|---|---|---|---|---|---|
| CV joint | −3.0 | 288.63 | 358.10 | 173.90 | 63.82 |
| | −1.5 | 297.00 | 362.40 | 194.40 | 56.57 |
| | 0.0 | 267.15 | 359.00 | 178.60 | 67.53 |
| | +1.5 | 266.68 | 340.40 | 87.30 | 94.91 |
| | +3.0 | 264.78 | 357.50 | 155.20 | 76.40 |
| **Mean** | | **276.85** | **355.48** | **157.88** | **71.84** |
| Watt's linkage | −3.0 | 171.29 | 356.00 | 0.00 | 207.83 |
| | −1.5 | 192.47 | 349.00 | 0.00 | 181.33 |
| | 0.0 | 185.27 | 359.00 | 21.00 | 182.44 |
| | +1.5 | 172.92 | 354.00 | 2.00 | 203.56 |
| | +3.0 | 149.71 | 351.00 | 6.00 | 230.45 |
| **Mean** | | **174.33** | **353.80** | **5.80** | **201.12** |
| Schmidt coupling | −3.0 | 253.68 | 314.50 | 198.62 | 45.68 |
| | −1.5 | 224.61 | 271.60 | 185.55 | 38.31 |
| | 0.0 | 255.67 | 323.10 | 191.94 | 51.30 |
| | +1.5 | 262.41 | 314.90 | 203.60 | 42.41 |
| | +3.0 | 257.40 | 360.70 | 173.07 | 72.89 |
| **Mean** | | **250.75** | **316.96** | **190.56** | **50.12** |

**Table 3.** Angular velocity and velocity ripple at five hub vertical offsets. Mean ripple ± standard error of the mean across the five offsets: CV joint 71.84 ± 6.6%, Watt's linkage 201.12 ± 9.1%, Schmidt coupling 50.12 ± 6.1%.

Figure 3 shows the trend of the data with error bars. The Schmidt coupling has lower values than the CV joint at all offsets, and the Watt's linkage has consistently higher values than the other two. The difference between the Watt linkage and the other two is large compared to the error bars. Meanwhile, the difference between the Schmidt coupling and the CV joint is smaller, and the error bars overlap at +3.0 cm.

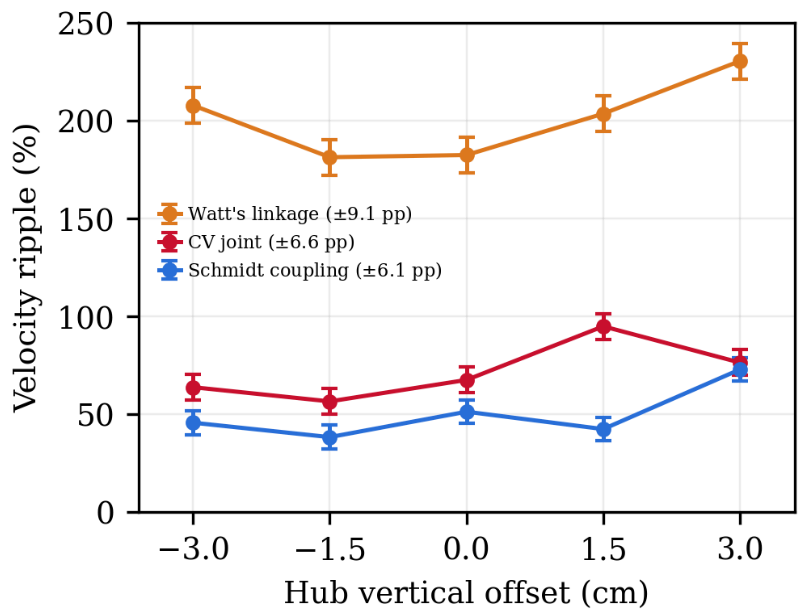


**Figure 3.** Output velocity ripple as a function of hub offset for the three mechanisms. The Schmidt coupling had the lowest ripple at all offsets while the geared Watt's linkage had the highest by more than 180% at all offsets. Error bars show the standard error of the mean for the five offsets used in each mechanism.

*3.2. Transmission efficiency*

Table 4 shows the corresponding stall-mass readings, torque computed in (2), gear ratios of each mechanism, and efficiency predicted by (5). The torque was acquired from the input side five times, and the average value is 0.4286 Nm.

| **Mechanism** | **Offset (cm)** | **Mass (kg)** | **Force (N)** | **Arm (m)** | **Torque (N·m)** | ***G*** | **η (%)** |
|---|---|---|---|---|---|---|---|
| Input (motor) | −3.0 | 0.810 | 7.938 | 0.050 | 0.3969 | — | — |
| | −1.5 | 0.930 | 9.114 | 0.050 | 0.4557 | — | — |
| | 0.0 | 0.853 | 8.359 | 0.050 | 0.4180 | — | — |
| | +1.5 | 0.920 | 9.016 | 0.050 | 0.4508 | — | — |
| | +3.0 | 0.860 | 8.428 | 0.050 | 0.4214 | — | — |
| **Mean** | | **0.875** | **8.571** | **0.050** | **0.4286** | **—** | **—** |
| CV joint | −3.0 | 0.304 | 2.979 | 0.075 | 0.2234 | 1.000 | 52.14 |
| | −1.5 | 0.301 | 2.950 | 0.075 | 0.2212 | 1.000 | 51.62 |
| | 0.0 | 0.326 | 3.195 | 0.075 | 0.2396 | 1.000 | 55.91 |
| | +1.5 | 0.315 | 3.087 | 0.075 | 0.2315 | 1.000 | 54.02 |
| | +3.0 | 0.297 | 2.911 | 0.075 | 0.2183 | 1.000 | 50.94 |
| **Mean** | | **0.309** | **3.024** | **0.075** | **0.2268** | **1.000** | **52.93** |
| Watt's linkage | −3.0 | 1.052 | 10.310 | 0.075 | 0.7732 | 8.000 | 22.55 |
| | −1.5 | 1.102 | 10.800 | 0.075 | 0.8100 | 8.000 | 23.63 |
| | 0.0 | 1.162 | 11.388 | 0.075 | 0.8541 | 8.000 | 24.91 |

| Mechanism | Offset (cm) | Mass (kg) | Force (N) | Arm (m) | Torque (N·m) | *G* | η (%) |
|---|---|---|---|---|---|---|---|
| | +1.5 | 1.082 | 10.604 | 0.075 | 0.7953 | 8.000 | 23.20 |
| | +3.0 | 1.096 | 10.741 | 0.075 | 0.8056 | 8.000 | 23.50 |
| **Mean** | | **1.099** | **10.769** | **0.075** | **0.8076** | **8.000** | **23.56** |
| Schmidt coupling | −3.0 | 0.292 | 2.862 | 0.075 | 0.2146 | 1.000 | 50.08 |
| | −1.5 | 0.322 | 3.156 | 0.075 | 0.2367 | 1.000 | 55.23 |
| | 0.0 | 0.325 | 3.185 | 0.075 | 0.2389 | 1.000 | 55.74 |
| | +1.5 | 0.301 | 2.950 | 0.075 | 0.2212 | 1.000 | 51.62 |
| | +3.0 | 0.331 | 3.244 | 0.075 | 0.2433 | 1.000 | 56.77 |
| **Mean** | | **0.314** | **3.079** | **0.075** | **0.2309** | **1.000** | **53.89** |

**Table 4.** Torque measurements and transmission efficiency.

Figure 4 shows the mean efficiency by mechanism with standard-error bars. The CV joint and Schmidt coupling have overlapping confidence intervals, whereas the Watt's linkage has a much lower efficiency, being less than half the mean efficiency of the other two mechanisms.

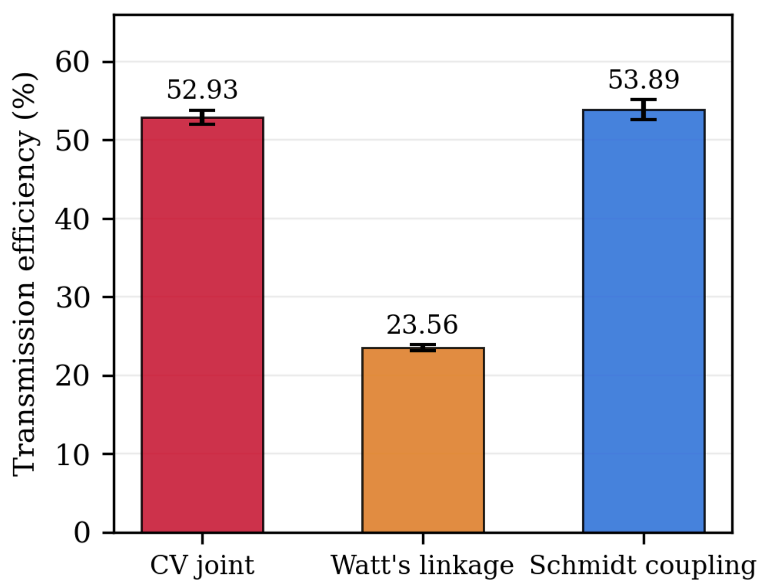


**Figure 4.** Mean transmission efficiency by mechanism. Error bars show the standard error of the mean transmission efficiency, calculated over the five measured hub offsets.

### *3.3. Statistical comparison*

All pairwise comparisons were made with Welch's two-sample *t*-tests across the five hub offsets ($n$ = 5 per mechanism). The results are shown in Table 5.

| Measure | Comparison | Difference | *t* | *p* |
|---|---|---|---|---|
| Velocity ripple | Schmidt vs. CV | −21.72 pp (30.2% rel.) | −2.42 | 0.042 |
| Velocity ripple | Schmidt vs. Watt's | −151.00 pp (75.1% rel.) | −13.81 | $< 10^{-5}$ |

| Measure | Comparison | Difference | *t* | *p* |
|---|---|---|---|---|
| Velocity ripple | CV vs. Watt's | −129.28 pp (64.3% rel.) | −11.51 | $< 10^{-5}$ |
| Efficiency | Schmidt vs. CV | +0.96 pp (1.8% rel.) | 0.61 | 0.560 |
| Efficiency | Schmidt vs. Watt's | +30.33 pp (128.8% rel.) | 22.57 | $< 10^{-5}$ |
| Efficiency | CV vs. Watt's | +29.37 pp (124.7% rel.) | 29.84 | $< 10^{-5}$ |

**Table 5.** Welch's two-sample t-tests for all pairwise comparisons.

## 4. Discussion

### *4.1. Efficiency*

The Schmidt coupling had a mean efficiency of 53.89% compared to 52.93% of the CV joint, which is a difference of 0.96%. Using Welch's two sample t-test to test the five hub offsets gives us t = 0.61, p = 0.56. As such, the difference is not significant at any meaningful level, and the standard-error intervals in Figure 4 actually overlap. The correct conclusion is therefore not that the Schmidt coupling is significantly better than the CV joint, but rather that the two are statistically identical within the resolution of this experiment.

The geared Watt's linkage achieved only 23.56%, which is less than half of the efficiency of either of the alternatives. The reason behind this is the gear train, since the teeth of the gears interact by sliding contact; the printed teeth create additional friction, which the link-based counterparts do not possess. This explains why the play in the gear train is noticeable during the operation.

It is important to note that efficiency was calculated in terms of (5) instead of (3). If the efficiency was calculated in terms of power, then the efficiency of the Watt's linkage would be dependent on the hypothetical load at which the output shaft was rotating, and the comparison of the 1:1 and 8:1 systems would be based on this same hypothetical value. However, calculating efficiency in terms of torque, as given by (5), requires only the ratio of the kinematic pairs, which are defined by the number of teeth.

### *4.2. Velocity ripple*

The mean ripple for the Schmidt coupling was 50.12%, for the CV joint –71.84%, and for the Watt's linkage – 201.12%. Thus, the Schmidt coupling was found to be underperformed by 21.7 percentage points compared to the CV joint, which is a decrease by 30.2%. According to Welch's test, t = –2.42, p = 0.042, which is significant at 5% confidence level, although not very substantial. Compared to the Watt's linkage, the decrease was 151.0 percentage points, p < 10−5.

The difference between the mechanisms is explained by the contact types used to transmit rotation. The Schmidt coupling differs from the geared Watt's linkage in that the former transmits motion through link pivots that rotate relative to each other, whereas the latter uses teeth that engage with a variable geometry in the plane. In the Watt's linkage, the measured minimal velocity reached zero or a near-zero value for four out of five cases corresponding to a particular offset, suggesting that it came to a temporary halt or binding during reciprocating motion. As expected, the performance of the CV joint was intermediate between that of the other two mechanisms, which corresponded to the observation of Lee and Polycarpou (2010) that its friction increased with the degree of articulation.

*4.3. Relationship between the two measures*

The Watt's linkage performed worst on both measures, and the Schmidt coupling is the best, which suggests a common cause for the observed loss: the friction in the mechanism, which must be responsible for both effects. However, the agreement is not perfect, as the three mechanisms are separated in the rankings: on the ripple, on the top, from the middle, and on the bottom, while on the efficiency, the Schmidt coupling and the CV joint are equal ($p = 0.56$), so that the efficiency only distinguishes between two levels. There is no obvious connection between the two, as there was no variation in friction as a separate factor, which could be said to affect both.

*4.4. Limitations*

Sample size is the main issue. Each mechanism was tested only once for each of the five hub offsets. Position was an independent variable, and so the study varied position rather than repeating trials at the same position. As such, repeatability was not formally assessed, and error bars and t-tests conflate position effects with trial-to-trial repeatability within a position. A proper repeatability study would entail measuring one mechanism several times at the same offset, and would be an informative addition to this study. It would also reduce the error bars on the ripple, which are currently barely significant (0.10). The sample was made of 3D-printed polymers. Machined metals would have been a better choice, as finer machining would lead to higher measured efficiency and lower measured ripple due to reduced friction and backlash. The relative ordering of the three mechanisms would likely remain the same, but their separation would be smaller, as the printed teeth produce more penalty on the geared mechanism than on the link mechanisms. The torque was measured at stall, rather than at a continuously driven torque. Stall torque is simple to measure and has good repeatability, but represents a different operating regime to the one experienced by a suspension mechanism, which is always moving. Finally, the hub was positioned at an offset for each measurement, rather than being moved through the offset during the measurement. The behavior of the mechanism during traversal of an offset is different from its behavior at any given offset.

Three drives for transmitting torque from a moving parallel offset were built to the same wheel hub geometry, driven from one input, and tested at five wheel hub vertical offsets. The Schmidt coupling decreased the mean output velocity ripple by from 71.84% to 50.12% compared to the CV joint, which was statistically significant at the 5% level ($p = 0.042$). The Schmidt coupling had a transmission efficiency of 53.89%, compared to 52.93% for the CV joint, which was not significantly different ($p = 0.56$); there is no measurable benefit for using the Schmidt coupling in terms of transmission efficiency. Lastly, the geared Watt's linkage was considerably worse in both categories at 201.12% velocity ripple and 23.56% efficiency.

Link-based parallel-offset couplings like the Schmidt coupling can therefore transmit drive torque to a wheel hub through the suspension travel with less torque ripple than a CV-joint and similar efficiency. This allows retaining the motor at the chassis while restoring in-hub packaging advantage, thus addressing the main concern about unsprung mass and making the wheel integrated drive more viable. However, this is only a proof of concept due to the small data set, paper prototyping, and static loading.

Additional work includes testing the mechanisms at the full suspension travel with an in-wheel motor mounting, rebuilding the device with metal parts, and investigating other kinds of parallel-offset couplings such as the Oldham coupling.

## Statements and declarations

*Disclosure of interest*

The authors report there are no competing interests to declare.

*Use of AI Statement*

During the preparation of this work, the authors used Claude (Anthropic) to assist with data processing code. The authors reviewed and edited the output as needed and take full responsibility for the content of the published article.

*Funding*

The author(s) received no financial support for the research, authorship, and/or publication of this article.

*Data availability statement*

Raw Tracker output for all fifteen runs, giving tracked position against time at 240 frames/s, is available from the corresponding author on request. Computer-aided design models and data acquisition code are also available on request.

*Author contributions*

B.S.: Conceptualization; Methodology; Investigation; Formal analysis; Data curation; Software; Visualization; Writing – original draft; Writing – review and editing.

C.S.: Conceptualization; Methodology; Investigation; Formal analysis; Data curation; Software; Visualization; Writing – original draft; Writing – review and editing.

## References

Deepak, K., M. A. Frikha, Y. Benômar, M. El Baghdadi, and O. Hegazy. 2023. "In-wheel motor drive systems for electric vehicles: State of the art, challenges, and future trends." *Energies* 16 (7): 3121. doi:10.3390/en16073121.

Deo, H. V., and N. P. Suh. 2004. "Axiomatic design of automobile suspension and steering systems: Proposal for a novel six-bar suspension." SAE Technical Paper 2004-01-0811. Warrendale, PA: SAE International. doi:10.4271/2004-01-0811.

Hunt, K. H. 1973. "Constant-velocity shaft couplings: A general theory." *Journal of Engineering for Industry* 95 (2): 455–64. doi:10.1115/1.3438177.

Hyundai Motor Group. 2023. "The universal wheel drive system, a paradigm shift in drive systems." Accessed March 27, 2026. https://www.hyundaimotorgroup.com/en/story/CONT0000000000125025.

Lee, C. H., and A. A. Polycarpou. 2010. "A phenomenological friction model of tripod constant velocity (CV) joints." *Tribology International* 43 (4): 844–58. doi:10.1016/j.triboint.2009.12.004.

Mackey, J., S. Goldsack, and S. Dick. 2017. "Next-generation in-wheel electric hub drives." SAE Technical Paper 2024-01-3626. Warrendale, PA: SAE International. doi:10.4271/2024-01-3626.

Xu, X., M. Wang, P. Xiao, J. Ding, and X. Zhang. 2023. "In-wheel motor control system for four-wheel drive electric vehicle based on CR-GWO-PID control." *Sensors* 23 (19): 8311. doi:10.3390/s23198311.

Zhai, R., P. Xiao, R. Zhang, and J. Ju. 2022. "In-wheel motor control system used by four-wheel drive electric vehicle based on whale optimization algorithm-proportional–integral–derivative control." *Advances in Mechanical Engineering* 14 (6): 16878132221104574. doi:10.1177/16878132221104574.